BJPS

Brazilian Journal of Pharmaceutical Sciences

http://dx.doi.org/10.1590/s2175-97902022e19922

Article

Zofenopril antitumor activity in mice bearing Ehrlich solid carcinoma: Modulation of PI3K/AKT signaling pathway

Suzan Mohamed Mansour[1,2*], Rasha Youssef Mohammed Ibrahim[3]

[1]Department of Pharmacology and Toxicology, Faculty of Pharmacy, Cairo University, Cairo, Egypt, [2]Department of Pharmacology, Toxicology and Biochemistry, Faculty of Pharmacy, Future University in Egypt, Cairo, Egypt, [3]Department of Radioisotopes, Nuclear Research Centre, Atomic Energy Authority, Cairo, Egypt

Angiotensin-II (AgII) is thought to be crucial for tumor growth and progression. Moreover, hydrogen sulfide (H_2S) performs a controversial action in cancer pathology. Zofenopril (ZF) is an angiotensin-converting enzyme (ACE) inhibitor with H_2S donating properties. Hence, this study aims at investigating the tumor suppressor activity of ZF and elucidating the involved trajectories in Ehrlich's solid tumor (EST)-bearing mice. EST was induced by the intradermal injection of Ehrlich's ascites carcinoma cells into femoral region. All parameters were assessed after 28 days post-inoculation or one-week thereafter. ZF treatment resulted in significant reduction of tumor weights with marked decrease in IL-6 and VEGF levels in serum, and tumor Ag II and CEA contents. Additionally, the administration of ZF downregulated the tumor gene expression of cyclin-D, ACE-1, and Bcl2 and upregulated the proapoptotic gene, BAX. Moreover, ZF increased CBS gene expression, which is a major contributor to cellular H_2S production. In addition, ZF was able to reduce the protein expression of PI3K, *p*AKT, *p*GSK-3β, and NFκB. Our study has provided novel insights into the possible mechanisms by which ZF may produce its tumor defeating properties. These intersecting trajectories involve the interference between PI3K/Akt and CBS signaling pathways.

Keywords: Zofenopril. Angiotensin II. Cancer. PI3K/Akt. Hydrogen sulfide. Cystathionine beta synthase.

INTRODUCTION

Angiotensin-II (Ag-II) is a key member of the renin angiotensin system (RAS) that is well known for its impacts on blood pressure control, vascular remodeling, angiogenesis, and inflammation. The components of RAS are upregulated in assortment of tumors involving breast (Rodrigues-Ferreira *et al.,* 2012), endometrial (Nowakowska *et al.,* 2016), lung (Cortez-Retamozo *et al.,* 2013) and prostate (Dominska *et al.,* 2017), affirming the important role of Ag-II in tumor progression and metastasis (Zhang,Wang, 2018). Ag-II expression is related to expanded protein tyrosine phosphorylation and activation of the mitogen-activated protein kinases (MAPK), which prompts the instigation of growth factors and cytokines (Kim, Iwao, 2000; Touyz, Berry, 2002). Numerous studies have demonstrated that RAS blockade hampers tumor development both in vitro (Attoub *et al.,* 2008; Wilsdorf *et al.,* 2001) and in vivo (Miyajima *et al.,* 2002; Neo *et al.,* 2010, 2007). However, some other studies have proposed that this inhibition is due to halting angiogenesis.

Vascular Endothelial Growth Factor (VEGF) is the most powerful proangiogenic inducer that can activate phosphoinositide 3-kinase (PI3K)/ serine-threonine kinase-1 (Akt) signaling pathways after binding to its receptor tyrosine kinase to encourage tumor cell expansion, migration and angiogenesis (Yan *et al.,*

***Correspondence:** S. M. Mansour**.** 1 Department of Pharmacology and Toxicology**.** Faculty of Pharmacy**.** Cairo University, Cairo, Egypt**.** 2 Department of Pharmacology, Toxicology and Biochemistry**.** Faculty of Pharmacy**.** Future University in Egypt, Cairo, Egypt**.** E-mails: suzan.mansour@pharma.cu.edu.eg; suzan.mohamed@fue.edu.eg. Orcid ID: https://orcid.org/0000-0002-9235-7351. R. Y.M. Ibrahim. E-mail: drrashayoussef@yahoo.com

2019). The PI3K/Akt cascade is a main controller of cell survival and fate through various downstream cell targets. One of these targets is glycogen synthase kinase-3β (GSK3β), which results in upregulated cyclin D1 and Myc expression with considerable acceleration of cell cycle (Zhu *et al.,* 2011). NFκB is another key signaling element affected by PI3K/Akt incitement. Akt surges the degradation of the inhibitor of κB (IκB) with ensuing release of NFκB, which is pivotal in the commencement and progression of the disease, as well as development of aggressive tumors resisting the effect of various drugs (Ahmad *et al.,* 2013). Moreover, Akt can restrict cellular apoptosis and augment its survival through the deactivation of BAX and BAD, but it hoists the antiapoptotic B-cell lymphoma 2 (Bcl-2), Bcl-xl and myeloid cell leukemia 1 levels (Atif, Yousuf, Stein, 2015).

Zofenopril (ZF) is an angiotensin-converting enzyme (ACE) inhibitor with sulphydryl groups. It is characterized by high lipophilicity, high tissue penetration and powerful antioxidant effects (Napoli *et al.,* 2004). Studies have confirmed that hydrogen sulfide (H_2S) is engaged in the mechanisms by which ZF autonomously improves the vascular function and performs its ACE inhibiting activity (Bucci *et al.,* 2014; Donnarumma *et al.,* 2016; Monti *et al.,* 2016). Synthesis of H_2S occurs naturally from cysteine through some enzymes including cystathionine-c lyase (CSE), cystathionine β-synthetase (CBS) and 3-mercaptosulfurtransferase (3-MST). The role of CBS-triggered endogenous H_2S generation in cancer biology is disputable. On one hand, at low H_2S levels, it has been proved that it aids tumor development by keeping up mitochondrial respiration and production of ATP, invigorating proliferation and survival, as well as, redox balance and vasodilation (Zhu *et al*., 2018). On the other hand, at higher concentrations, it works as a mitochondrial toxin by hampering cytochrome c oxidase with subsequent antitumor activity (Szabo *et al.,* 2013b).

In light of the previous background, the present study has been carried out to explore the potential tumor suppressing ability of ZF in Ehrlich solid tumor (EST)-bearing mice. The study was also extended to elucidate some of the possibly involved trajectories that could be responsible for the obtained antitumor activity.

MATERIAL AND METHODS

Material

Animals

Male Swiss albino mice, weighing 20–30 g, were used in the present study. They were obtained from the animal house of the National Cancer Institute, Cairo, Egypt. Mice were housed in polyethylene cages under controlled laboratory conditions (25 ± 1°C temperature, constant relative humidity and normal dark/light cycle). They were acclimatized to the experimental conditions for at least 1 week prior to the start of the experiment. Animals were allowed free access to standardized laboratory balanced diet and water. The study was carried out under strict conditions in accordance with the recommendations of the Guide for the Care and Use of Laboratory Animals of the National Institutes of Health (NIH publication No.85-23, 1996). The protocol was revised and approved by the Ethics Research Committee of Faculty of Pharmaceutical Sciences and Pharmaceutical Industries, Future University in Egypt (REC-FPSPI-12/85). All efforts were exerted to minimize animal suffering during the experimental period. The duration of the experiment was as short as possible, and the number of animals was kept to a minimum. Unnecessary disturbance of animals was avoided. Tough maneuver was avoided, and all animals were sacrificed by an overdose of thiopental.

Drugs and Chemicals

Zofenopril calcium (ZF) was purchased from Sigma Aldrich®, MO, USA. ZF was kept at 2-8°C and freshly dissolved in saline. The concentration was adjusted so that each 10 g animal body weight would receive 0.1 ml solution. All other chemicals were of analytical grade or equal quality.

Methods

Ehrlich tumor cells inoculation

Mice were injected with fixed number of Ehrlich's ascites carcinoma (EAC) cell line (0.2 mL EAC cells containing 2 x 10^6 cells/ mouse) suspended in saline. EAC cell line was obtained from the Tumor Biology Department, National Cancer Institute, Cairo University (Cairo, Egypt). They were prepared under sterile conditions. The viability of EAC cell line was tested using Trypan blue dye exclusion technique. Tumors were induced by intradermal injection into the femoral region of the recipient male mouse. Tumors were left for 7–10 days to grow big as its diameter achieved 0.7–1.2 cm (Abd-Alhaseeb *et al.,* 2014; Calixto-Campos *et al.,* 2013).

Experimental design

Animals were initially weighed and randomly divided into five groups (n=10): (1) Normal-Control group; (2) Positive-Control group (EST-bearing mice); (3) ZF-Control group received ZF (15 mg/kg/day; p.o.) for 1 month; (4) ZF-Protection group that administered ZF (15 mg/kg/day; p.o.) from the day of EAC cells inoculation (day 1) until the end of experiment on day 30; (5) ZF-Treatment group given ZF (15 mg/kg/day; p.o.) form day 7 of EAC cells inoculation to the end of the experiment on day 37.

By the end of the experiment, animals were weighed to estimate % weight gain, which was calculated using the following formula: (([final body weight - initial body weight]/ intial body weight) *100). Blood samples were withdrawn from each mouse from the orbital sinuses. Blood samples were allowed to stand for 15 min. at room temperature and then centrifuged at 3000 g for 10 min. Serum samples were then separated and stored at -80°C till used for biochemical parameters determination. Mice were sacrificed by a lethal dose injection of thiopental. Tumor discs were isolated from inoculated mice viz; groups 2, 4 and 5. The discs were weighed and processed for histopathological or molecular biology studies.

Biochemical studies

The serum levels of interleukin-6 (IL-6), vascular endothelial growth factor (VEGF) and angiotensin-II (Ag-II) were determined using ELISA kits according to the manufacturer's instructions using monoclonal antibodies specific for mouse IL-6 and VEGF (R&D Systems, USA) and Ag-II (Sigma-Aldrich, Germany). The color intensity was measured at 450 nm using a microplate reader (Bio Tek Instruments, VT, USA). On the other hand, the level of carcinoembryonic antigen (CEA) was measured by a radioimmunoassay method using commercially available kits (Immunotech. A Beckman Coulter/ Ref.2121).

Quantitative real-time (qRT-PCR)

Total RNA Isolation system (Promega, Madison, WI, USA) was used for total RNA extraction from tumor tissues using SV and the purity of obtained RNA was verified spectrophotometrically at 260 nm. The extracted RNA was reverse transcribed into cDNA using RT-PCR kit (Stratagene, Santa Clara, CA) according to the manufacturer's instructions. To assess the expression of the target genes, quantitative real-time PCR was performed using SYBR green PCR Master mix (Qiagen, Germany) as described by the manufacturer. Briefly, 25µL of QuntiFast SYBR Green PCR Master Mix, 22.5µL dH2O, 2µL primer pair mix (5 pmol/µL each primer), and 0.5µL cDNA to reach a final reaction volume of 50µL. The sequences of primers (ThermoFisher Scientific, MA, USA) of BAX, Bcl2, ACE-1, cyclin-D, CBS and housekeeping gene (β-actin) are listed in Table I. PCR reactions included 10 min at 95 °C for the activation of AmpliTaq DNA polymerase, followed by 40 cycles at 95°C for 15 s (denaturing) and 60°C for 1 min (annealing/extension). The data were expressed in cycle threshold (C_t), where the increased fluorescence curve passes across a threshold value. The relative expression of the target gene was obtained using the comparative C_t ($\Delta\Delta C_t$) method. The ΔC_t was calculated by subtracting BAX, Bcl2, ACE-1, cyclin-D or CBS C_t from that of target gene, whereas $\Delta\Delta C_t$ was obtained by subtracting the ΔC_t of reference sample (internal control) from that of test sample. The relative expression ratios were calculated by the $2^{-\Delta\Delta C_t}$ (Pfaffl, 2001).

Table I - Primer sequences for qRT-PCR.

Gene	Sequences
BAX	Forward 5`-CCC TGT GCA CTA AAG TGC CC-3` Reverse 5`- CTT CTT CAC GAT GGT GAG CG-3`
Bcl2	Forward 5`-CTA CGA GTG GGA TGC TGG AG-3` Reverse 5`-GGT CAG ATG GAC ACA TGG TG-3`
ACE-1	Forward 5`-CCA CCG TTA CCA GAC AAC TAT CC-3` Reverse 5`-GCG TAT TCG TTC CAC AAC ACC T-3`
Cyclin-D1	Forward 5'TGGAGCCCCTGAAGAAGAG-3' Reverse 5'AAGTGCGTTGTGCGGTAGC-3'
CBS	Forward primer :5'-CGG ATC CAC ACGN GACT CTT-3' Reverse primer:5′-GGA ATT CCA ATAG GAC CAGC ACGA TC-3`
β-actin	Forward primer: 5' ATC CGT AAA GAC CTC TAT GC 3' Reverse primer: 5' AAC GCA GCT CAG TAA CAG TC 3'

Western blot analysis

Following tumor protein quantification (Bio-Rad Protein Assay Kit, CA, USA), 10 µg protein of each sample were separated by SDS polyacrylamide gel electrophoresis and transferred to a nitrocellulose membrane using a semi-dry transfer apparatus (Bio-Rad, CA, USA). Membranes were then soaked in 5% non-fat dry milk to block non-specific binding sites. Later, the membrane was incubated with anti-*p*Akt (1:1000; cat#: 44-621G), anti-PI3K (1:500; cat#: MA5-17150), anti-NF-κB p-65 (cat#: PA1-186), anti-T-GSK3β (1:250; cat#: 39-9500), anti-*p*GSK3β (1:1000; cat#: MA5-14873) (ThermoFisher Scientific, MA, USA) overnight at 4˚C on a roller shaker. The membranes were then probed with horseradish peroxidase-conjugated goat anti-rat immunoglobulin (Dianova, Hamburg, Germany). Finally, the blots were developed with enhanced chemiluminescence detection reagent (Amersham Biosciences, IL, USA). The protein was quantified by densitometric analysis using a scanning laser densitometer (GS-800 system, Bio-Rad, CA, USA). The results were expressed as arbitrary units (AU) after normalization for β-actin protein expression.

Histopathological examinations

The tumor samples were fixed in 10% phosphate buffered formaldehyde. Subsequently, all the specimens were washed in tap water for half an hour and then dehydrated using ascending grades of alcohol (70%, 80%, 90% and finally absolute alcohol). The specimens were then cleared in xylene, impregnated in soft paraffin wax at 55ºC and embedded in hard paraffin. Sections of 6 µm thickness were cut using a slide microtome and then stained with hematoxylin and eosin (Bancroft, Gamble, 2008). Six random non overlapping fields were scanned and analyzed for the assessment of mean area % of necrotic tissue per tissue section of each sample. All obtained data and micrographs were analyzed by using Leica application module (Leica Microsystems GmbH, Germany) for tissue sections analysis. Moreover, scoring for tumor sections was carried out to determine tumor cells pleomorphism, newly formed blood vessels, inflammatory cells infiltration and skeletal muscle damage. The severity of these alterations was represented as: + mild, ++ moderate and +++ severe. All histopathological examinations were performed by an experienced pathologist who was blinded to the experimental groups.

Statistical methods

Data are expressed as mean ± standard error (SE). All statistical analyses were performed using Version 6 (GraphPad Software Inc., CA, USA). The comparison among groups was performed by using One-way ANOVA followed by Tukey as a post hoc test at $p< 0.05$.

RESULTS

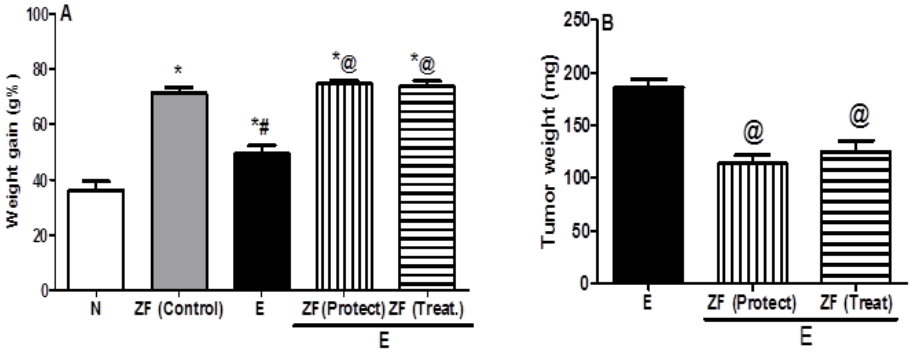

FIGURE 1 - *Effect of ZF on percentage body weight gain and tumor weight*

As depicted by Figure 1A, the administration of ZF to the normal mice resulted in marked increase in % body weight gain. On the other hand, the EST-bearing mice showed significant reduction in % body weight gain, as compared to the normal-control group. The treatment of tumor-bearing mice with ZF starting from the first day (Protection Group) of EAC inoculation or the first week (Treatment Group) thereafter markedly raised % body weight gain, as compared to the EST-control group.

Regarding the effect on tumor weight, Figure 1B showed that the administration of ZF to both protection and treatment groups significantly reduced tumor weight, as compared to the EST-control mice.

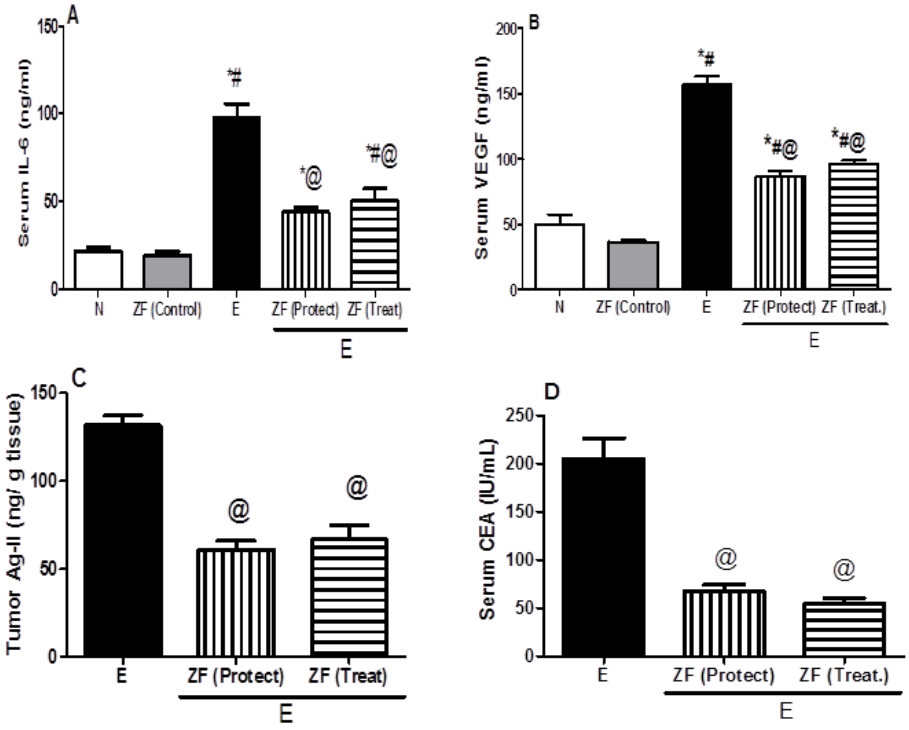

FIGURE 2 - *Effect of ZF on serum levels of IL-6 and VEGF, as well as, Ag-II and CEA tumor levels*

As demonstrated in Figure 2, IL-6 and VEGF levels in serum were obviously greater in the EST-control mice, as compared to the normal ones. However, the treatment with ZF starting from the first day of EAC inoculation or the first week thereafter significantly reduced their levels, as compared to the EST-control mice (Figure 2A & 2B).

Similarly, the administration of ZF starting from first day of EAC inoculation or the first week thereafter resulted in pronounced reduction of tumor Ag-II and CEA contents, as compared to the EST-control mice (Figure 2 C & D).

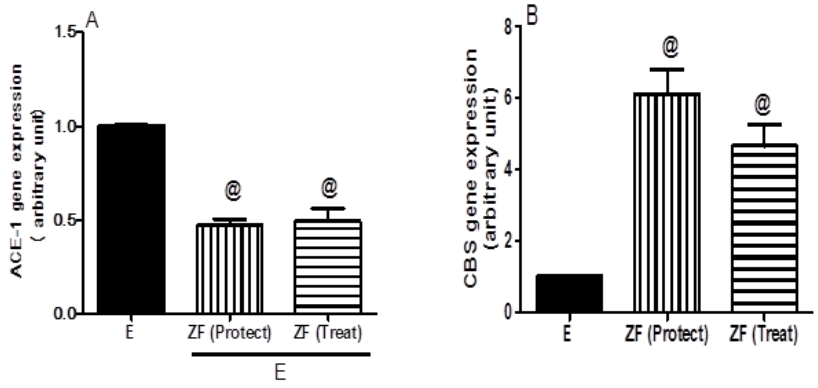

FIGURE 3 - *Effect of ZF on intratumoral gene expression of ACE-1 and CBS*

ACE-1 gene expression was significantly reduced following the administration of ZF either starting from the first day of EAC inoculation or the first week thereafter, as compared to the EST-control mice (Figure 3 A).

On the other hand, the treatment with ZF markedly elevated intratumoral CBS gene expression of EST-bearing mice, as compared to the EST-control ones (Figure 3B).

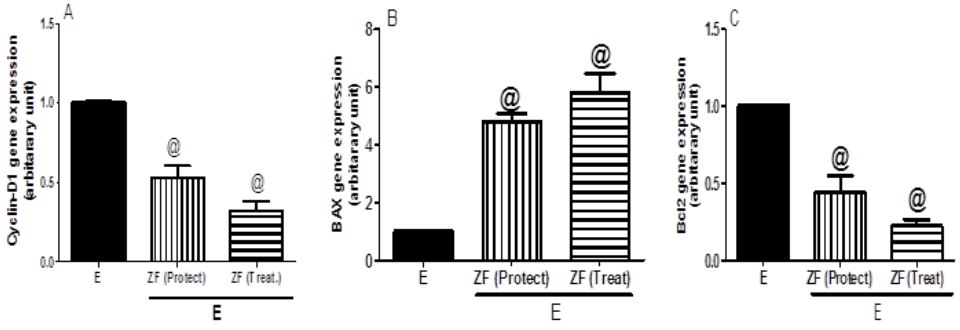

FIGURE 4 - *Effect of ZF on intratumoral gene expression of cyclin-D, BAX and Bcl2*

Cyclin-D and Bcl2 gene expression were markedly decreased after the administration of ZF either starting from the first day of EAC inoculation or the first week thereafter, as compared to the EST-control mice (Figure 4A & 4C).

However, the treatment with ZF effectively increased intratumoral BAX gene expression of EST-bearing mice, as compared to the EST-control ones (Figure 4B).

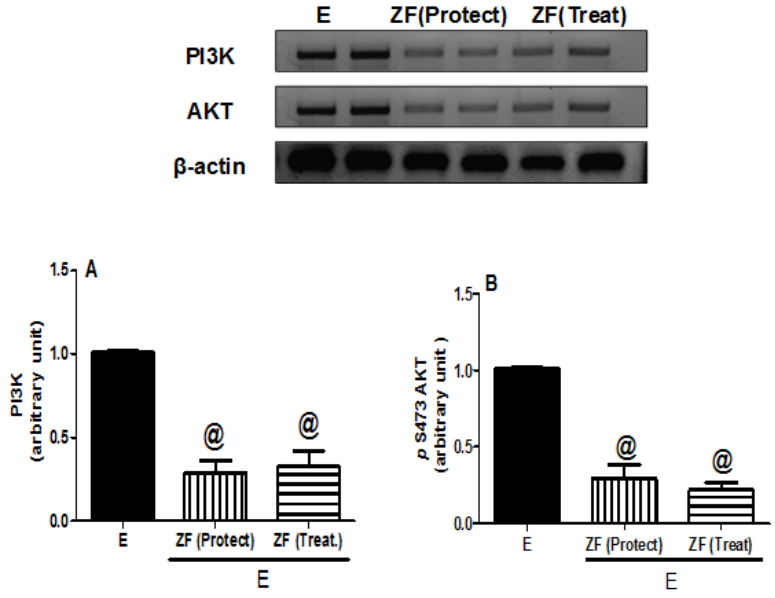

FIGURE 5 - *Effect of ZF on intratumoral protein expression of PI3K and p-(S473) Akt*

As depicted in Figure 5, the administration of ZF in both treatment regimens suppressed the intratumoral protein expression of PI3K and p-Akt, as compared to EST-bearing mice.

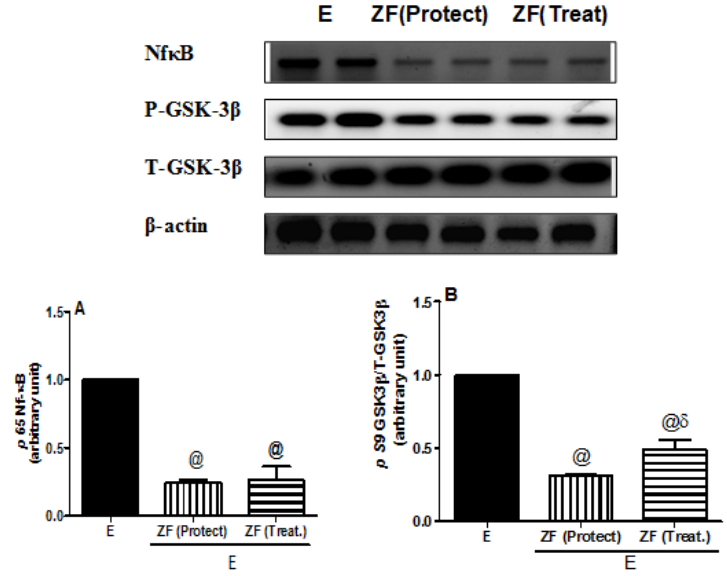

FIGURE 6 - *Intratumoral protein expression of p-(S9) GSK-3β and p 65 NfκB*

Figure 6 shows that the treatment with ZF for 1 month either from the first day of EAC inoculation or the first week thereafter significantly reduced the intratumoral protein expression of p-GSK-3β and NfκB, as compared to EST-bearing mice.

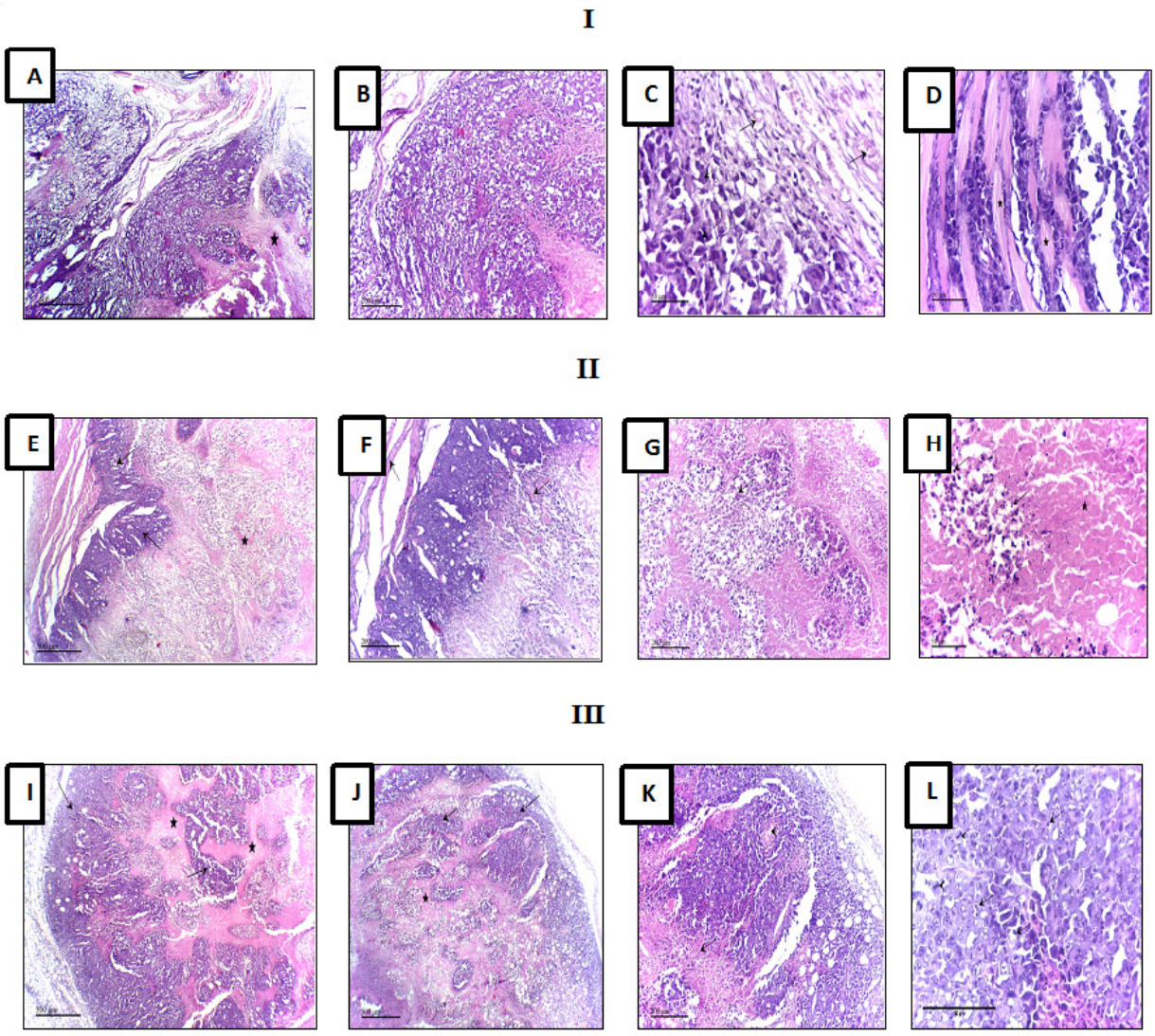

FIGURE 7 - *Effect on tumor histopathological examination*

The histopathological findings demonstrated in Figure 7 show that EST-bearing control mice have extensive subcutaneous infiltration of viable tumor cells [A], with marked pleomorphism, anaplasia [B] and newly formed blood vessels with hyperchromatsia [C], in addition to massive infiltration of viable tumor cells between degenerated skeletal muscle fibers [D].

On the other hand, the administration of ZF starting from the day of EAC inoculation resulted in marked reduction in tumor mass as manifested by wide diffuse areas of necrotic tumor tissue with smaller areas of inflammatory cells [E], [G] and [H], in addition to intact skeletal muscle fibers in the outer tumor zones [F].

The treatment of EST-bearing mice with ZF starting from 7th day post-inoculation resulted in moderate reduction in tumor mass as demonstrated by the wider outer viable zone of tumor cells with diffuse areas of necrotic tissue in the deeper zones with viable sheets of tumor cells with many small blood vessels [I] and [J]. Many of tumor cells showed 1 or 2 prominent nucleoli with many mitotic figures and few scattered lymphocytes [K] and [L]. These data are summarized in Table II.

Table II - Effect of oral administration of zofenopril (15 mg/kg/day) on severity of histopathological alterations in tumors isolated from EST-bearing mice

	E	ZF (Protect)	ZF (Treat.)
Tumor cells pleomorphism	+++	++	+++
Newly formed blood vessels	+++	+	++
Inflammatory cells infiltration	++	+	+
Skeletal muscle damage	+++	+	++

where +++ severe, ++ moderate, + mild

DISCUSSION

This investigation affords novel insights into the antitumor activity of ZF in EST-bearing mice. ESTs are quite similar to human tumors and are utilized in numerous investigations as experimental models to examine the antitumor activity of drugs or natural compounds. In this regard, the results of this work have shown that the administration of ZF starting from the 1st day of tumor inoculation or one week thereafter resulted in marked reduction in tumor masses with wide diffuse areas of necrosis. Such findings are consistent with some other findings reached by many authors who confirmed the central role of RAS in cancer pathology and the anticancer activity of drugs causing RAS blockade (Abd-Alhaseeb *et al.,* 2014; Araújo *et al.,* 2015; Zhang,Wang, 2018).

The increased expression of Ag-II is in part associated with the release of inflammatory cytokines such IL-6 (Nakaigawa *et al.,* 2006; Nakamura *et al.,* 2018) and NfκB (Zhao *et al.,* 2014) and the rise in tyrosine phosphorylation is associated with ensuing instigation of growth factors such as VEGF (Abd-Alhaseeb *et al.,* 2014; Nakamura *et al.,* 2018). They were all reported to promote chief components in cancer pathology. We found that administration of ZF was accompanied by marked reduction in serum levels of Ag-II and VEGF, and intratumoral gene expression of NfκB as well.

Besides, the current work has demonstrated that the administration of ZF resulted in significant decrease in phosphorylation of PI3K and Akt with consequent reduction in their downstream signaling pathways including GSK-3β, NfκB and cyclin-D. The PI3K/Akt signaling cascade is believed to stand out amongst chief oncogenic trajectories in human malignancy. An increasing body of evidence has shown that this pathway is commonly hyperactivated in many cancer types (Crowell, Steele, Fay, 2007; Song *et al.,* 2019). PI3K transmits impulses from various growth factors, cytokines and oncoproteins to multiple targets including Akt, which in turn, controls various cellular functions, including cell survival, proliferation and development (Crowell, Steele, Fay, 2007). GSK-3β, a serine/threonine kinase is phosphorylated and deactivated by Akt that accordingly augments cyclin D1 and Myc expression (Zhu *et al.,* 2011). In addition, Akt-induced suppression of forkhead box O1 (FOXO1) diminishes p27 and p21 levels and sequentially enhanced cyclin-dependent kinase expression. Consequently, the enhancement of these molecules significantly encouraged progression of the cell cycle. Hence, inhibiting the PI3K/Akt signaling trajectories could be one of the imperative factors by which ZF produces its antitumor activity.

Moreover, NfκB is an additional signaling molecule activated by Akt. It is crucial for the initiation and progress of cancers, and for gaining of drug resistance in aggressive cancers (Ahmad *et al.,* 2013b; Zhang *et al.,* 2015). Once NFκB turns free under the influence of Akt, it can quickly translocate to the nucleus and trigger the transcription of several target genes. Moreover, Akt may hamper cellular programmed cell death. It is able to debilitate pro-apoptotic Bad and Bax activities, and strengthen anti-apoptotic Bcl2, Bcl-xl though (Atif, Yousuf, Stein, 2015). Thus, the global power of PI3K/Akt signaling is about enhancing cellular replication and survival and lessening apoptosis, that are in whole hallmarks for carcinogenesis. ZF was able to suppress PI3K/Akt signaling cascade either directly by inhibiting their trajectories or indirectly by inhibiting ACE-1 with subsequent reduction in Ag-II, cytokines such as IL-6 or growth factors like VEGF.

Another prime target that may explain the observed tumor suppressing activity of ZF is its H_2S donating

properties. Supporting body of evidence has proposed the association of H_2S as yet another mechanism by which ZF improves peripheral vascular function (Bucci *et al.,* 2014). Our findings showed that ZF use was accompanied by marked increase in intratumoral CBS gene expression, a key enzyme involved in H2S biosynthesis, suggesting a pronounced increase in intratumoral H_2S contents. Diminished CBS activity was also reported in a mouse-hepatocellular carcinoma tumor model (Avila *et al.,* 2000). However, it is now obvious that CBS activity plays a controversial role in cancer pathology. Under normal circumstances, CBS-prompted endogenous H_2S production was accounted to support tumor growth by preserving mitochondrial respiration and ATP synthesis, and to stimulate cell proliferation and survival *(Lagoutte et al.,* 2010; Szabo *et al.,* 2013a). Additionally, H_2S may stimulate cellular replication through augmentation of specific kinase pathways such as PI3K/Akt (CAI *et al.,* 2007; Manna, Jain, 2011). Further, H_2S induces the sulfhydration of NFκB, which appeared to repress apoptosis and might be of specific importance to cancer cell growth and survival (Sen *et al.,* 2012).

Despite what might be expected, at higher concentrations, H_2S goes about as a mitochondrial poison by means of the concealment of cytochrome c oxidase in mitochondrial complex IV. Additional cytotoxic effects may involve calcium and iron mobilization, mitochondrial uncoupling, pore opening, DNA damage, release of excitatory amino acids and intracellular acidification (Szabo *et al.,* 2013b). H_2S-donating compounds, such as sulfhydryl ACEI as ZF possess biphasic response, deliver H_2S exogenously in which low H_2S levels boost cellular proliferation and cell viability. However, high H_2S concentrations cause malicious/unfavorable impacts in cells (Hellmich *et al.,* 2015; Szabo *et al.,* 2013b). Our findings have demonstrated that ZF upregulated CBS intratumoral gene expression, confirming the significant rise in intratumoral H_2S contents with subsequent cytotoxicity.

In conclusion, this study has highlighted the beneficial tumor defeating properties of ZF. Such favorable effects could be achieved via modulating the crosstalk between PI3K/Akt and H_2S signaling pathways. Further investigations are however necessary to determine the likelihood of incorporating ZF in the treatment of malignant tumors.

DISCLOSURE OF POTENTIAL CONFLICT OF INTEREST

None of the authors have any conflict of interests to declare.

REFERENCES

Abd-Alhaseeb MM, Zaitone SA, Abou-El-Ela SH, Moustafa YM. Olmesartan potentiates the anti-angiogenic effect of sorafenib in mice bearing ehrlich's ascites carcinoma: role of angiotensin (1–7). PLoS One. 2014;22:9(1):e85891.

Ahmad A, Biersack B, Li Y, Kong D, Bao B, Schobert R, et al. Targeted regulation of PI3K/Akt/mTOR/NF-κB signaling by indole compounds and their derivatives: mechanistic details and biological implications for cancer therapy. Anticancer Agents Med Chem. 2013;13(7):1002-1013.

Araújo WF, Naves MA, Ravanini JN, Schor N, Teixeira VPC. Renin-angiotensin system (RAS) blockade attenuates growth and metastatic potential of renal cell carcinoma in mice. Urol. Oncol. 2015;33(9):389.e1-7

Atif F, Yousuf S, Stein DG. Anti-tumor effects of progesterone in human glioblastoma multiforme: Role of PI3K/Akt/mTOR signaling. J Steroid Biochem Mol Biol. 2015;146:62–73.

Attoub S, Gaben AM, Al-Salam S, Al Sultan MAH, John A, Nicholls MG, et al. Captopril as a potential inhibitor of lung tumor growth and metastasis. Ann N Y Acad Sci. 2008;1138:65–72.

Avila MA, Berasain C, Torres L, Martín-Duce A, Corrales FJ, Yang H, et al. Reduced mRNA abundance of the main enzymes involved in methionine metabolism in human liver cirrhosis and hepatocellular carcinoma. J Hepatol. 2000;33(6):907–914.

Bancroft JD, Gamble M. Theory and practice of histological techniques. 2008; Churchill Livingstone/Elsevier.

Bucci M, Vellecco V, Cantalupo A, Brancaleone V, Zhou Z, Evangelista S, et al. Hydrogen sulfide accounts for the peripheral vascular effects of zofenopril independently of ACE inhibition. Cardiovasc Res. 2014;102(1):138–147.

CAI W, WANG M, MOORE P, JIN H, YAO T, ZHU Y. The novel proangiogenic effect of hydrogen sulfide is dependent on Akt phosphorylation. Cardiovasc Res. 2007;76(1):29–40.

Calixto-Campos C, Zarpelon AC, Corrêa M, Cardoso RDR, Pinho-Ribeiro FA, Cecchini R, et al. The ehrlich tumor induces pain-like behavior in mice: a novel model of cancer pain for pathophysiological studies and pharmacological screening. Biomed Res Int. 2013;2013:624815.

Cortez-Retamozo V, Etzrodt M, Newton A, Ryan R, Pucci F, Sio SWW, et al. Angiotensin II drives the production of tumor-promoting macrophages. immunity. 2013;38(2):296–308.

Crowell JA, Steele VE, Fay JR. Targeting the AKT protein kinase for cancer chemoprevention. Mol Cancer Ther. 2007;6(8):2139–2148.

Dominska K, Kowalska K, Matysiak ZE, Płuciennik E, Ochędalski T, Piastowska-Ciesielska AW. Regulation of mRNA gene expression of members of the NF-κB transcription factor gene family by angiotensin II and relaxin 2 in normal and cancer prostate cell lines. Mol Med Rep. 2017;15(6):4352–4359.

Donnarumma E, Ali MJ, Rushing AM, Scarborough AL, Bradley JM, Organ CL, et al. Zofenopril protects against myocardial ischemia-reperfusion injury by increasing nitric oxide and hydrogen sulfide bioavailability. J Am Heart Assoc. 2016;5(7):1–17.

Hellmich MR, Coletta C, Chao C, Szabo C. The therapeutic potential of cystathionine β-synthetase/hydrogen sulfide inhibition in cancer. Antioxid Redox Signal. 2015;22(5):424–448.

Kim S, Iwao H. Molecular and cellular mechanisms of angiotensin II-mediated cardiovascular and renal diseases. Pharmacol Rev. 2000;52(1):11–34.

Lagoutte E, Mimoun S, Andriamihaja M, Chaumontet C, Blachier F, Bouillaud F. Oxidation of hydrogen sulfide remains a priority in mammalian cells and causes reverse electron transfer in colonocytes. Biochim Biophys Acta - Bioenerg. 2010;1797(8):1500–1511.

Manna P, Jain SK. Hydrogen Sulfide and l-Cysteine Increase Phosphatidylinositol 3,4,5-Trisphosphate (PIP3) and Glucose Utilization by Inhibiting Phosphatase and Tensin Homolog (PTEN) Protein and Activating Phosphoinositide 3-Kinase (PI3K)/Serine/Threonine Protein Kinase (AKT)/Protein Kinase Cζ/λ (PKCζ/λ) in 3T3l1 Adipocytes. J Biol Chem. 2011;286(46):39848–39859.

Miyajima A, Kosaka T, Asano T, Asano T, Seta K, Kawai T, et al. Angiotensin II type I antagonist prevents pulmonary metastasis of murine renal cancer by inhibiting tumor angiogenesis. Cancer Res. 2002;62(15):4176–9.

Monti M, Terzuoli E, Ziche M, Morbidelli L. H 2 S dependent and independent anti-inflammatory activity of zofenoprilat in cells of the vascular wall. Pharmacol Res. 2016;113(Pt A):426–437.

Nakaigawa N, Sasaki T, Ishiguro H, Kubota Y, Uemura H, Kato S, et al. Antiproliferative activity of angiotensin II receptor blocker through cross-talk between stromal and epithelial prostate cancer cells. Mol Cancer Ther. 2006;4(11):1699–1709.

Nakamura K, Yaguchi T, Ohmura G, Kobayashi A, Kawamura N, Iwata T, et al. Involvement of local renin-angiotensin system in immunosuppression of tumor microenvironment. Cancer Sci. 2018;109(1):54–64.

Napoli C, Sica V, de Nigris F, Pignalosa O, Condorelli M, Ignarro L, et al. Sulfhydryl angiotensin-converting enzyme inhibition induces sustained reduction of systemic oxidative stress and improves the nitric oxide pathway in patients with essential hypertension. Am Heart J. 2004;148(1):172.

Neo JH, Ager EI, Angus PW, Zhu J, Herath CB, Christophi C. Changes in the renin angiotensin system during the development of colorectal cancer liver metastases. BMC Cancer. 2010;10:134.

Neo JH, Malcontenti-Wilson C, Muralidharan V, Christophi C. Effect of ACE inhibitors and angiotensin II receptor antagonists in a mouse model of colorectal cancer liver metastases. J Gastroenterol Hepatol. 2007;22(4):577–584.

Nowakowska M, Matysiak-Burzyńska Z, Kowalska K, Płuciennik E, Domińska K, Piastowska-Ciesielska AW. Angiotensin II promotes endometrial cancer cell survival. Oncol Rep. 2016;36(2):1101–1110.

Pfaffl MW. A new mathematical model for relative quantification in real-time RT-PCR. Nucleic Acids Res. 2001;29(9):e45.

Rodrigues-Ferreira S, Abdelkarim M, Dillenburg-Pilla P, Luissint A-C, Di-Tommaso A, Dé Rique Deshayes F, et al. Angiotensin II facilitates breast cancer cell migration and metastasis. Angiotensin II facil. Breast Cancer Cell Migr. Metastasis. PLoS ONE. 2012;7(4):e35667.

Sen N, Paul BD, Gadalla MM, Mustafa AK, Sen T, Xu R, et al. Hydrogen sulfide-linked sulfhydration of NF-κB mediates its antiapoptotic actions. Mol Cell. 2012;45(1):13–24.

Song M, Bode AM, Dong Z, Lee M.-H. AKT as a therapeutic target for cancer. Cancer Res. 2019;79(6):1–14.

Szabo C, Coletta C, Chao C, Módis K, Szczesny B, Papapetropoulos A, et al. Tumor-derived hydrogen sulfide, produced by cystathionine-β-synthase, stimulates bioenergetics, cell proliferation, and angiogenesis in colon cancer. Proc Natl Acad Sci USA. 2013a;110(30):12474–12479.

Szabo C, Ransy C, Módis K, Andriamihaja M, Murghes B, Coletta C, et al. Regulation of mitochondrial bioenergetic function by hydrogen sulfide. Part I. Biochemical

and physiological mechanisms. Br J Pharmacol. 2013b;171(8):2099-2122.

Touyz RM, Berry C. Recent advances in angiotensin II signaling. Braz J Med Biol Res. = Rev Bras Pesqui Medicas Biol. 2002;35(9):1001–1015.

Wilsdorf T, Gainer JV, Murphey LJ, Vaughan DE, Brown NJ. Angiotensin-(1-7) does not affect vasodilator or TPA responses to bradykinin in human forearm. Hypertens. 2001;37(4):1136–40.

Yan X, Hui Y, Hua Y, Huang L, Wang L, Peng F, et al. EG-VEGF silencing inhibits cell proliferation and promotes cell apoptosis in pancreatic carcinoma via PI3K/AKT/mTOR signaling pathway. Biomed Pharmacother. 2019;109:762–769.

Zhang J, Yu XH, Yan YG, Wang C, Wang WJ. PI3K/Akt signaling in osteosarcoma. Clin Chim Acta. 2015;444:182–192.

Zhang S, Wang Y. Telmisartan inhibits NSCLC A549 cell proliferation and migration by regulating the PI3K/AKT signaling pathway. Oncol Lett. 2018;15(4):5859–5864.

Zhao Y, Wang H, Li X, Cao M, Lu H, Meng Q, et al. Ang II-AT1R increases cell migration through PI3K/AKT and NF-κB pathways in breast cancer. J Cell Physiol. 2014;229(11):1855–1862.

Zhu H, Blake S, Chan KT, Pearson RB, Kang J. Cystathionine ß-synthase in physiology and cancer. Biomed Res Int. 2018;3205125.

Zhu Q, Yang J, Han S, Liu J, Holzbeierlein J, Thrasher JB, et al. Suppression of glycogen synthase kinase 3 activity reduces tumor growth of prostate cancer in vivo. Prostate. 2011;71(8):835–845.

Received for publication on 13rd November 2019
Accepted for publication on 23rd April 2020